

**$^{93}\text{Nb}$  NMR study of disorder in  $\text{KTa}_{1-x}\text{Nb}_x\text{O}_3$** S. Rankel, B. Zalar, V. V. Laguta,\* and R. Blinc  
*J. Stefan Institute, Ljubljana, Slovenia*J. Toulouse  
*Lehigh University, Bethlehem, Pennsylvania 18015, USA*  
(Received 19 October 2004; published 22 April 2005)

The  $^{93}\text{Nb}$  nuclear magnetic resonance spectra of a mixed  $\text{KTa}_{1-x}\text{Nb}_x\text{O}_3$  (KTN) single crystal with  $x=15\%$  have been measured. The observation of an unresolved quadrupole-induced first-order satellite background below the sharp central  $1/2 \leftrightarrow -1/2$  transition already in the cubic phase demonstrates that the Nb ions are dynamically disordered between off-center positions rather than being located at the high symmetry central perovskite site. The angular dependence of the second moment of the satellite background further shows that these distortions and the biasing of the Nb hopping are of rhombohedral symmetry, i.e., the Nb ions are effectively displaced along the  $[111]$  body diagonals. The two-order-of-magnitude difference between the spin-lattice ( $T_1$ ) and spin-spin ( $T_2$ ) relaxation times indicates a two-time scale behavior: the faster time scale can be tentatively assigned to biased hopping of the Nb ion and the slower one to flipping of rhombohedral nanodomains which percolate at the ferroelectric transition. This also agrees with the observed huge increase in the second moment  $M_2$  at the transition to the ferroelectric phase at  $T_C=135$  K.

DOI: 10.1103/PhysRevB.71.144110

PACS number(s): 76.60.-k, 61.46.+w

**INTRODUCTION**

Potassium tantalate,  $\text{KTaO}_3$ , is considered to be a quantum paraelectric, the ferroelectricity of which is suppressed by quantum fluctuations.<sup>1,2</sup> It has a cubic perovskite structure all the way down to the lowest temperatures measured. Potassium niobate,  $\text{KNbO}_3$ , on the other hand, is ferroelectric up to 700 K. The mixed system  $\text{KTa}_{1-x}\text{Nb}_x\text{O}_3$  (KTN) exhibits a ferroelectric transition for  $x \geq 0.8\%$ . The transition temperature  $T_C$  varies<sup>3</sup> with  $x$  as  $T_C \propto (x-x_C)^{1/2}$ . The dopant Nb is replacing Ta and has been supposed to occupy the central Ta site with a negligible ionic size misfit.

KTN was considered to be a ferroelectric solid solution until Samara<sup>4</sup> discovered glassy type dielectric dispersion upon hydrostatic pressure. He concluded that the Nb ions under pressure were off center for times up to milliseconds and that they formed clusters with distributed relaxation times. At ambient pressure (1 bar) the Nb should be static and off center. According to a recent study of the same author<sup>5</sup> Nb is actually not static but hops between off-center positions. A number of experiments<sup>6,7</sup> indicate that at lower temperatures the motion of the niobium ions becomes correlated and polar nanoregions form. Dielectric dispersion in the kHz–MHz range was observed by Sommer *et al.*<sup>8</sup> and a strong frequency dependence of the hysteresis loops by Knauss *et al.*<sup>9</sup> indicating relaxor behavior. Local distortions were also inferred from the observation of first order Raman scattering lines.<sup>10</sup> Extended x-ray absorption fine structure (EXAFS) data<sup>11</sup> have now convincingly shown that the Nb ions should be off center in a sample containing 9% Nb.

A model was recently proposed<sup>12</sup> describing the evolution of Nb correlations, suggesting in particular the existence of a two time-scale dynamics.

Van der Klink *et al.*<sup>13</sup> observed by nuclear magnetic resonance (NMR) that the  $^{93}\text{Nb}$  ( $I=9/2$ ) satellites are wiped out

in a mixed KTN crystal and concluded that Nb fluctuates around the central position at a rate exceeding  $10^4 \text{ s}^{-1}$  above  $T_C$  whereas it stays off center for a longer time below  $T_C$ . This was later confirmed by a study of the effect of the polarization fluctuations on the elastic constants. In this study, Knauss *et al.*<sup>6</sup> showed that the coupling of polarization fluctuations (from hopping Nb ions) to acoustic waves could be turned off or enhanced by the application of appropriately oriented dc electric fields. Rod *et al.*<sup>14</sup> suggested that polarization fluctuation clouds form and from the width of the  $^{93}\text{Nb}$  NMR central transition follows an estimate for the maximum  $^{93}\text{Nb}$  second order shift, which gives an upper limit of  $\delta < 0.15 \text{ \AA}$ . They stated that this shift is nonzero within a time interval up to 100 ns.<sup>14</sup> The  $^{93}\text{Nb}$  spin-lattice relaxation rate shows a maximum at  $T_C$  as expected for a classical ferroelectric. It should be noted that well-resolved Nb satellites were observed in pure  $\text{KNbO}_3$  in the ferroelectric phase.<sup>15</sup> The quadrupole coupling in  $\text{KNbO}_3$  is huge, indicating a sizeable off-center shift of the Nb ion. In the room temperature orthorhombic phase, the Nb quadrupole coupling constant  $e^2qQ/h$  is 23.5 MHz and the asymmetry parameter of the electric field gradient (EFG) tensor is  $\eta = 0.8$ .

In spite of many investigations, the origin of the Nb off center shifts and the Nb dynamics in KTN are still not well understood.

To throw additional light on the microscopic nature of the Nb off center shifts and disorder in KTN, we decided to study the angular dependence of the quadrupole perturbed  $^{93}\text{Nb}$  NMR spectra of a KTN single crystal doped with 15% Nb. We used the “exorcycle” pulse sequence appropriate for the study of satellites with minimal signal distortions. This sequence has been recently used in the  $^{47}\text{Ti}$  and  $^{49}\text{Ti}$  NMR of  $\text{BaTiO}_3$  (Ref. 16) to detect the first order satellite background, demonstrating the existence of off-center Ti sites in the high temperature cubic phase.

We particularly hoped to see whether above  $T_C$  the Nb ion occupies the central position with occasional fluctuations around this position or whether it is disordered between off-center sites. In the first case the Nb quadrupole coupling should be zero by symmetry whereas it should be nonzero in the second case.

We also wanted to check if the off centering of the niobium is static—as first suggested by Samara<sup>4</sup> and the EXAFS data<sup>9</sup>—or dynamic. In case of static Nb off-center sites, well resolved first order satellites should be observable. If however the disorder among off-center sites is dynamic, the satellites should be broadened or smeared out.

### EXPERIMENT

The  $^{93}\text{Nb}$  ( $I=9/2$ ) NMR spectra were measured at a Larmor frequency  $\omega_L/2\pi=92.917\,400$  MHz corresponding to a magnetic field 9.2 T. The KTN single crystal had a  $T_C \approx 135$  K and was doped with 15% Nb.

The sample dimensions were  $5.5\text{ mm} \times 8\text{ mm} \times 3\text{ mm}$  with the surfaces parallel to the crystallographic (010) planes. The sample [100] axis was perpendicular to the external magnetic field and the sample was rotated around the axis [100] by an angle  $\vartheta$ .

The two pulse, four phase ( $xx, xy, x-x, x-y$ ) “exorcycle” pulse sequence was used to avoid signal distortions. The length of the  $\pi/2$  pulse was typically  $2\ \mu\text{s}$ . The spin-spin relaxation time  $T_2$  was determined by fitting multiple exponentials to the decay of the signal vs pulse separation  $\tau$  at various frequency offsets. The spin-lattice relaxation time  $T_1$  was measured by the saturation recovery techniques.

### RESULTS AND DISCUSSION

The  $^{93}\text{Nb}$  NMR spectra in the cubic phase at 290 K, and in the rhombohedral phase at 80 K, are presented in Fig. 1. The line shape is a two-component one. It exhibits a sharp central line and a broad background. The line shapes are very close to those observed for  $^{47}\text{Ti}$  and  $^{49}\text{Ti}$  NMR in the cubic phase of  $\text{BaTiO}_3$ .<sup>16</sup> By analogy with the case of Ti in  $\text{BaTiO}_3$ , we can assign the broad background component to unresolved or poorly resolved first order satellites,  $\pm 1/2 \leftrightarrow \pm 3/2$ ,  $\pm 3/2 \leftrightarrow \pm 5/2$ ,  $\pm 5/2 \leftrightarrow \pm 7/2$ , and  $\pm 7/2 \leftrightarrow \pm 9/2$ , and the central sharp component to the  $1/2 \leftrightarrow -1/2$  transition, which is not affected by quadrupole coupling in first order.

The frequency shift

$$\Delta\nu_m = \nu_{m-1 \leftrightarrow m} - \nu_L \quad (1)$$

of the  $m-1 \leftrightarrow m$  transition with respect to the Larmor frequency  $\nu_L$  is given, in first order, by

$$\Delta_m = -\nu_Q \left(m - \frac{1}{2}\right) (3 \cos^2 \theta - 1 + \eta \sin^2 \theta \cos 2\phi) / 2, \quad (2)$$

where  $\nu_Q = 3K/[2I(2I-1)]$  denotes the quadrupole frequency. Here  $K = e^2qQ/h$  is the quadrupole coupling constant. It is related to the largest eigenvalue  $V_{zz} = eq$  of the EFG tensor, which, according to the point charge model, is proportional to the square of the off-center shift of the Nb ion.  $\eta = (V_{xx} - V_{yy})/V_{zz}$  is the asymmetry parameter of this tensor.  $\theta$  and  $\phi$

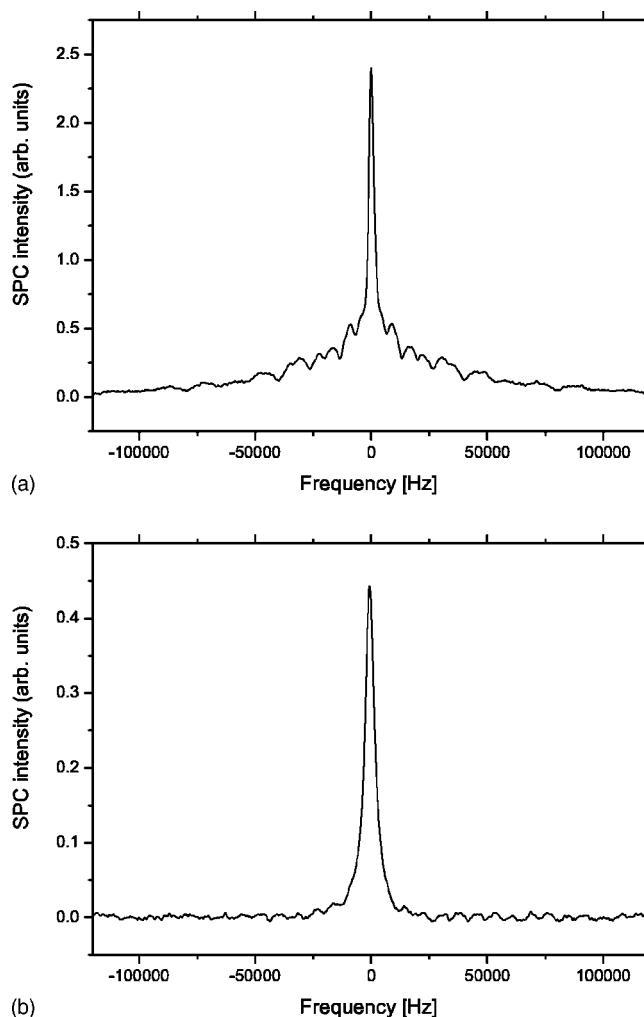


FIG. 1.  $^{93}\text{Nb}$  NMR spectra of  $\text{KTa}_{0.85}\text{Nb}_{0.15}\text{O}_3$  in the high temperature cubic phase at 290 K and low temperature ferroelectric phase at 80 K.

are the tilt and azimuthal angles of the direction of the external magnetic field  $B$  with respect to the EFG tensor eigenframe. Thus  $\phi$  and  $\theta$  are the first two Euler angles of the  $x$ -convention matrix  $R(\phi, \theta, \psi)$  (Ref. 17) that describes the rotation of the crystal frame with respect to the laboratory frame  $XYZ$ , i.e., the rotation of the crystal in the external magnetic field  $B_0 \parallel Z$ . As the NMR response is invariant to rotations of the sample about any axis parallel to  $B_0$ , frequency shift does not depend on the third Euler angle  $\psi$ .

The central line shifts in second order only. For  $\eta=0$ , the shift is given by

$$\nu_{1/2 \leftrightarrow -1/2} = \frac{-\nu_Q^2}{16\nu_L} (a - 3/4)(1 - \cos^2 \theta)(9 \cos^2 \theta - 1), \quad (3)$$

$$a = I(I + 1).$$

The integral intensities of the central component and the broad background component are in the ratio 0.15, as predicted by theory.<sup>16</sup>

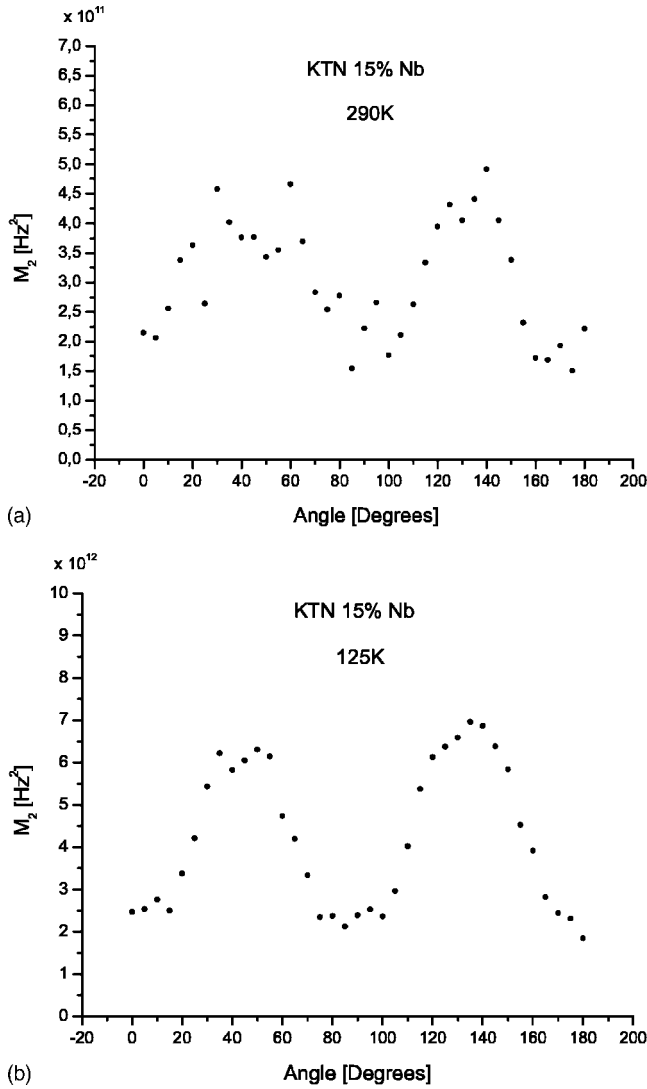


FIG. 2. Angular dependence of the second moment  $M_2$  in the high temperature cubic phase at 290 K and the tetragonal ferroelectric phase at 125 K for a rotation  $[100]$  perpendicular to  $\mathbf{B}_0$ .

This demonstrates that the broad background component is indeed due to unresolved satellites. A nonzero electric field gradient (EFG) tensor thus exists at the Nb sites as a result of off-center displacements of the Nb ions in the cubic phase. Besides this contribution, it is important to note that imperfections in the crystal, created by impurity ions, strains, vacancies, interstitials, etc., will also produce an EFG. They will however only contribute to the isotropic background.

The dependences of the second moment of the satellite background  $M_2(\vartheta)$  on the orientation of the crystal in the magnetic field in the high temperature cubic phase at 290 K and low temperature ferroelectric phase at 125 K are shown in Fig. 2.

In addition to an isotropic part we see a well-defined anisotropic part demonstrating local breaking of the symmetry of the high temperature cubic phase. Such an angular dependence should be absent for an EFG created by random imperfections.

The theoretical angular dependence of the second moment of the  $^{93}\text{Nb}$  satellite spectra for rhombohedral distortions is<sup>16</sup>

$$M_2(\vartheta) = M_2^0 + K^2 \frac{9(2I+3)(5+3\cos 2\vartheta)\sin^2 \vartheta}{640I^2(2I-1)}. \quad (4)$$

The observed angular dependence best agrees with rhombohedral distortions of the cubic symmetry due to Nb ion shifts along the body diagonals.

The calculations were made for the static case and averaged over all symmetry allowed domain orientations. Because of this averaging the first moment  $M_1$  does not depend on the orientation of the crystal.

It should be noted that the calculated angular dependence is also valid in the dynamic case where it appears as a prefactor in the spin-spin ( $T_2$ ) relaxation time.

Our results thus confirm that above  $T_C$  the equilibrium position of niobium is off-center along the body diagonals and that it is not occupying the central position even on the time average.

From the theoretical formula for the rhombohedral angular dependence of  $M_2$  and the experimental results we can obtain the values for the quadrupole coupling constant  $K$  and from it the  $^{93}\text{Nb}$  quadrupole frequency  $\nu_Q = 3K/2I(2I-1)$ . At room temperature in the cubic phase  $\nu_Q$  is 342 kHz. It increases to 1225 kHz below  $T_C$  at 125 K.

The off-center sites of the Nb ions are thus effectively displaced along the  $[111]$  directions, i.e., along the body diagonals, both at 290 K in the cubic phase and at 125 K in the distorted phase. This agrees with the EXAFS data. The Nb hopping is strongly biased, meaning that the Nb preferentially hops within a subset of its eight symmetry-related off-center positions. This, according to the Chaves model,<sup>18</sup> is what leads to local breaking of the cubic symmetry and the formation of differently oriented noncubic nanodomains as well as spatial disorder due to spatially varying orientations of the nanodomains (cf. Ref. 16). We thus have both dynamic disorder due to biased Nb hopping within a nanodomain (intersite hopping) and much slower fluctuations in the orientations of the nanodomains.

On cooling down from room temperature there is a small but significant shift  $\Delta\nu$  of the central  $\frac{1}{2} \leftrightarrow -\frac{1}{2}$  component line towards lower frequencies (Fig. 3) demonstrating an increase in the quadrupole frequency  $\nu_Q$ .

The shift of the central line is continuous in the cubic phase but exhibits a change in slope and a break at the transition to the ferroelectric tetragonal phase around  $T_C \approx 135$  K. Due to the increasing quadrupole coupling, the broad background component eventually moves out of the NMR observation window. Another change in the slope in the  $\Delta\nu$  vs  $T$  plot can be seen at the transition to the orthorhombic phase around 115 K.

The sequence of phase transitions in KTN is thus similar to the one in  $\text{BaTiO}_3$ . However, in contrast to  $\text{BaTiO}_3$ , the central  $\frac{1}{2} \leftrightarrow -\frac{1}{2}$  transition does not split at  $T_C$  [Fig. 4(a)] as would be expected if macroscopic  $90^\circ$  domains were to form in the tetragonal phase.<sup>16</sup> This demonstrates the presence of persisting disorder in the ferroelectric tetragonal phase, absent in  $\text{BaTiO}_3$ , as well as a large increase in the quadrupole coupling. The absence of a fully ordered ferroelectric phase in KTN below  $T_C$  is also seen in x-ray and neutron results, which do not show a splitting of the Bragg peaks but a very large increase in the Bragg intensity (relief of extinction).<sup>19</sup>

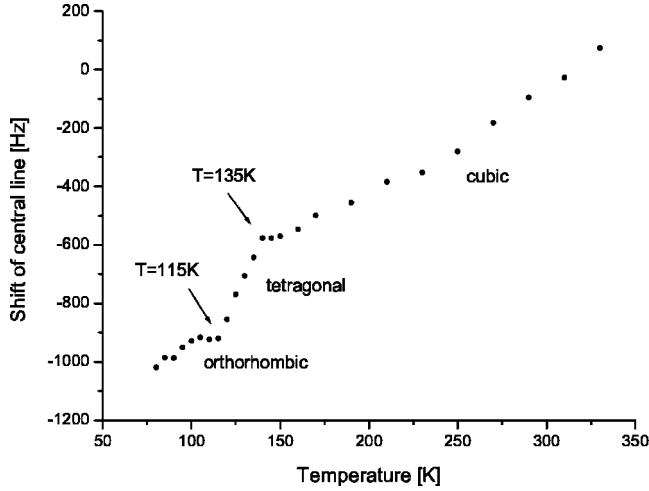


FIG. 3. Temperature dependence of the position of the central  $\frac{1}{2} \leftrightarrow -\frac{1}{2}$   $^{93}\text{Nb}$  NMR line relative to its position at 310 K.

Instead, there is a huge increase in the second moment of the Nb spectrum [Fig. 4(b)] below  $T_C$ .

The Nb quadrupole coupling frequencies  $\nu_Q$ , associated with the temperature dependence of the position of the central line and of the second moment, are several orders of magnitude lower than the frequencies of the dielectric relaxation mode ( $\sim 10^2$  MHz) associated with the hopping of the Nb ions among symmetry-related wells. The Nb NMR spectrum is thus observed in the limit of complete but biased motional narrowing. Incomplete restoration of the cubic symmetry and biased hopping can be directly inferred from the presence of the satellite background.

To further investigate the possible two-time scale dynamics of Nb mentioned above, we measured the temperature dependences of the Nb spin-lattice ( $T_1$ ) and spin-spin ( $T_2$ ) relaxation times (see Fig. 5). A two exponential magnetization recovery expected for the  $I=9/2$ , was observed. In agreement with the results of Rigamonti,<sup>20</sup> there is a dip in  $T_1$  at  $T_C$ . This implies a critical slowing down of the Nb intersite hopping, as expected at a ferroelectric phase transition.

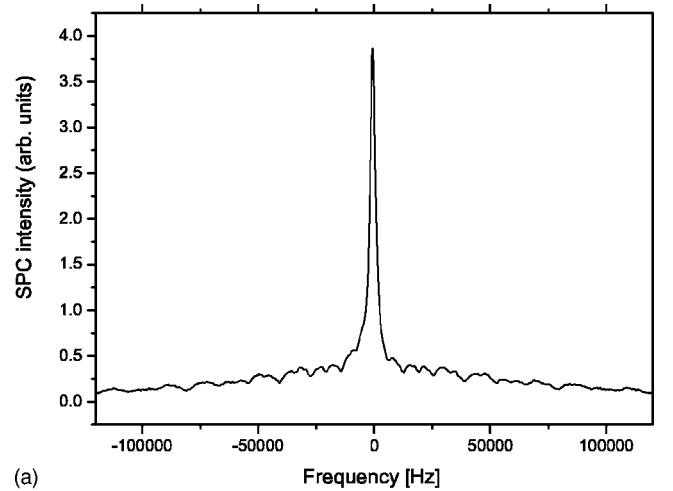
$T_2$  as well shows a dip at  $T_C$ . It is by two orders of magnitude shorter than  $T_1$ . This can be understood by examining the respective expressions for the two relaxation times.  $T_1$  is related to the spectral densities of the EFG tensor fluctuations  $J(\omega)$  at the Larmor frequency,  $\omega_L$ , and at twice the Larmor frequency,  $2\omega_L$ ,

$$\frac{1}{T_1} = [K_1 J(\omega_L) + K_2 J(2\omega_L)], \quad (5)$$

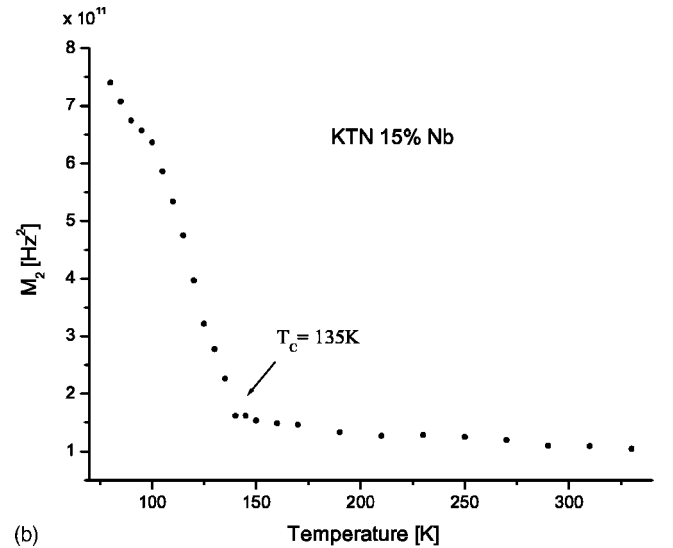
whereas the expression for  $T_2^{-1}$  of the satellite background contains an additional term<sup>21</sup> that is proportional to the spectral density at  $\omega=0$ , i.e., at very low frequencies,

$$\frac{1}{T_2} = [C_0 J(0) + C_1 J(\omega_L) + C_2 J(2\omega_L)]. \quad (6)$$

$C_0=0$  for the central  $\frac{1}{2} \leftrightarrow -\frac{1}{2}$  transition whereas it is nonzero for the satellite transitions.



(a)



(b)

FIG. 4. (a) The  $^{93}\text{Nb}$  NMR spectrum below  $T_C$  at 125 K (b) Temperature dependence of the second moment  $M_2$  of the  $^{93}\text{Nb}$  NMR spectrum showing a sudden increase at the transition to the ferroelectric phase at  $T_C \approx 135$  K.

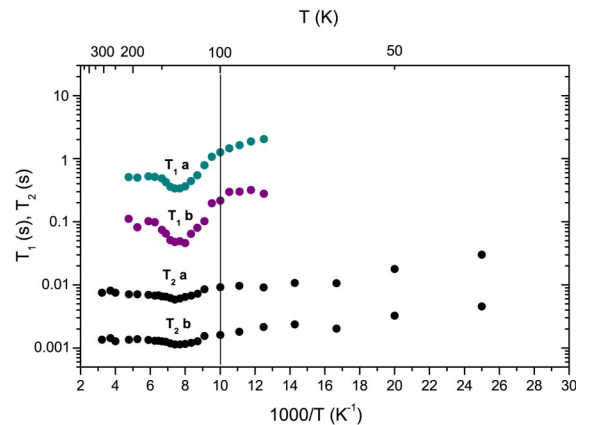


FIG. 5. (Color online) Temperature dependences of the  $^{93}\text{Nb}$  spin-lattice ( $T_1$ ) and spin-spin ( $T_2$ ) relaxation times in  $\text{KTa}_{0.85}\text{Nb}_{0.15}\text{O}_3$ .

Similarly to the case of  $\text{BaTiO}_3$  and PMN,<sup>16</sup> the motion measured by the  $J(0)$  term in KTN can be related to the flipping of nanodomains or the reorientation of polar nanoregions. However, the observed value of  $T_2$  in KTN is in the ms range and thus considerably longer than in  $\text{BaTiO}_3$ . It can account for part but not all of the satellite width. The homogeneous broadening is thus superimposed on an inhomogeneous broadening due to a disorder which is nearly static on the NMR time scale  $\tau_{\text{NMR}}^{-1} \approx \sqrt{M_2}$ .

### CONCLUSION

We have studied the quadrupole perturbed  $^{93}\text{Nb}$  NMR spectra of a KTN single crystal doped with 15% Nb. Measurements of the shift of the central line, the angular dependence of the second moment,  $M_2$ , the two relaxation times,  $T_1$  and  $T_2$ , and their temperature dependencies, show that, in KTN,

(i) Nb ions at all temperatures reside in off-center positions along  $[111]$  directions and the local breaking of the cubic symmetry is of rhombohedral nature;

(ii) The disorder is dynamic, i.e., the Nb ions undergo biased hopping within a subset of available symmetry-related off-center positions;

(iii) The Nb dynamics takes place on two very different time scales. On a short time scale, Nb undergoes rapid intersite biased hopping within individual nanodomains or polar nanoregions and, on a longer time scale, the orientations of these nanoregions fluctuate slowly. The flipping of the polar nanoregions, i.e., the noncubic nanodomains, is of the order of  $\tau_{\text{NMR}}^{-1}$ , whereas the Nb intersite hopping,  $\tau_{\langle 111 \rangle}^{-1}$ , is much faster,

$$\tau_{\langle 111 \rangle} \ll \tau_{\text{NMR}} \leq \tau_{\text{polar clusters}} \quad (7)$$

In contrast to the Nb intersite hopping, the flipping motion of the polar nanoregions is not critical at  $T_C$ . KTN with  $x = 15\%$  thus behaves as a “weak” relaxor undergoing a series of ferroelectric transitions in analogy to  $\text{BaTiO}_3$ . It exhibits both “order-disorder” and “displacive” components in the phase transition mechanism.

\*Permanent address: Institute for Problems of Materials Science, Ukrainian Academy of Sciences, Kiev, Ukraine.

<sup>1</sup>U. T. Höchli, H. E. Weibel, and L. A. Boatner, Phys. Rev. Lett. **39**, 1158 (1977).

<sup>2</sup>U. T. Höchli, Ferroelectrics **35**, 17 (1981).

<sup>3</sup>D. Rytz, U. T. Höchli, and H. Bilz, Phys. Rev. B **22**, 359 (1980).

<sup>4</sup>G. A. Samara, Phys. Rev. Lett. **53**, 298 (1984).

<sup>5</sup>G. A. Samara, J. Phys.: Condens. Matter **15**, R367 (2003).

<sup>6</sup>L. A. Knauss, X. M. Wang, and J. Toulouse, Phys. Rev. B **52**, 13 261 (1995).

<sup>7</sup>O. Svitelskiy, J. Toulouse, G. Yong, and Z.-G. Ye, Phys. Rev. B **68**, 104107 (2003).

<sup>8</sup>G. Hanskepetitpierre, E. A. Stern, and Y. Yacobi, J. Phys. (Paris) **47**, C8-675 (1986).

<sup>9</sup>D. Sommer, W. Kleemann, M. Lehdorff, and K. Dranstan, Solid State Commun. **72**, 731 (1989).

<sup>10</sup>L. A. Knauss, R. Pattnaik, and J. Toulouse, Phys. Rev. B **55**, 3472 (1997).

<sup>11</sup>P. DiAntonio, B. E. Vugmeister, J. Toulouse, and L. A. Boatner, Phys. Rev. B **47**, 5629 (1993).

<sup>12</sup>J. Toulouse, D. La-Orauttapong, and O. Svitelskiy, Ferroelectrics **302**, 271 (2004).

<sup>13</sup>J. J. Van der Klink, S. Rod, and A. Chatelain, Phys. Rev. B **33**, 2084 (1986).

<sup>14</sup>S. Rod, F. Borsa, and J. J. Van der Klink, Phys. Rev. B **38**, 2267 (1988).

<sup>15</sup>R. Kind, in *Magnetic Resonance and Related Phenomena*, Proceedings of the XVIIth Congress Ampere, Turku, Finland, 1972, edited by V. Hovi (North-Holland, Amsterdam, 1973).

<sup>16</sup>B. Zalar, V. V. Laguta, and R. Blinc, Phys. Rev. Lett. **90**, 037601 (2003).

<sup>17</sup>H. Goldstein, *Classical Mechanics* (Addison-Wesley, Reading, MA, 1980).

<sup>18</sup>A. S. Chaves, F. C. S. Barreto, R. A. Nogueira, and B. Zeks, Phys. Rev. B **13**, 207 (1976).

<sup>19</sup>P. M. Gehring, H. Chou, S. M. Shapiro, J. A. Hriljac, D. H. Chen, J. Toulouse, D. Rytz, and L. A. Boatner, Phys. Rev. B **46**, 5116 (1992).

<sup>20</sup>A. Rigamonti, Adv. Phys. **33**, 115 (1984).

<sup>21</sup>J. Seliger, J. Magn. Reson., Ser. A **116**, 67 (1995).